Serum Metabolic Profiling in a Mouse Model of Adriamycin-Induced Focal Segmental Glomerulosclerosis

Li Lyu[1], Cai-Li Wang[2], Zeng-Yan Li[2], Ying-Jin Shi[2], Yan-Hui Zhang[2], Yan Mi[2], Zhao Hu[1]

[1]Department of Nephrology, Qilu Hospital of Shandong University, Jinan, Shandong 250012, China

[2]Department of Nephrology, The First Affiliated Hospital of Baotou Medical College, Baotou, Inner Mongolia 014010, China

To the Editor: Focal segmental glomerulosclerosis (FSGS) is one of the leading causes of end-stage kidney disease.[1,2] However, no ideal intervention prevents FSGS progression due to the unclear physiopathological mechanisms. Adriamycin (ADR)-induced FSGS is a well-accepted model that mimics human FSGS. ADR, a common chemotherapeutic agent associated with nephrotoxicity, causes kidney damage by triggering imbalances between free oxygen radicals and antioxidant enzymes;[3-5] however, the precise mechanisms of ADR-induced FSGS are not completely clear. Metabolomics analysis is thought to be promising for monitoring treatment responses, making diagnoses, and tracking pathogenesis of diseases by assessing the end products of cellular processes and providing a nonbiased identification and quantification of all metabolites in a bioinformatics platform.[6] In the present study, we aimed to investigate serum metabolomic variations of ADR-induced FSGS model using ultra-performance liquid chromatography-mass spectrometry (UPLC-MS/MS) data collection technique. Here, we described the method of generating FSGS model using BALB/c mice in our laboratory. The clinical feature of ADR-induced FSGS was assessed by an increase in proteinuria, a rise in serum creatinine (SCR) and a loss of body weight. Serum and organs were harvested at 4 weeks after ADR administration, to assess kidney function, kidney pathological changes as well as serum metabolomic variations.

The mice were treated in accordance with guidelines approved by of The First Affiliated Hospital of Baotou Medical College. Due to the nephrotoxicity of ADR (doxorubicin hydrochloride; 10 mg/5 ml per vial as a stock solution, New York, USA), FSGS was developed as a metabolic-mediated chronic proteinuric renal disease. Twelve male BALB/c mice (average body weight 20 g, 8 weeks) were purchased from the Animal Center of Beijing, China, randomly divided into two groups (6 mice in each group: normal control and ADR-induced FSGS groups). These mice were fed in a dedicated animal research facility free of pathogens. The ADR-induced FSGS group (A group) was generated follows: the mice were given a slow tail vein injection of 10.5 mg/kg ADR in a 2 mg/ml solution at day 1. The tails were warmed under a lamp for 10 min, were useful for tail-vein dilatation before injection. The animals tolerated the ADR injections without significant immediate mortality; however, they ultimately developed kidney failure. The mice in the normal control group (C group) received an equal volume of 0.9% saline solution at the same time. One mouse injected with ADR died on day 22 and was not further considered in the subsequent study. The FSGS model was induced successfully at day 28. Body weights were measured, and urine samples were collected every week before and after administration. In brief, the process of urine collection was as follows: Urine samples were respectively collected from the normal control group and the ADR-induced FSGS group before administration of saline and ADR as well as on days 8, 15, 21, and 28. The mice were separately placed in a metabolism cage for the collection of urine. After a mouse urinated in a metabolism cage, the urine was collected with a micropipette. This process was repeated until a total volume of 100 μl had been collected. After collection, all urine samples were centrifuged (10,000 ×*g*, 10 min) and stored at −80°C until use. All mice were sacrificed at day 29 to evaluate the effects of ADR.

Urinary protein was measured and normalized with the bicinchoninic acid (BCA, Beyotime Ltd., Jiangsu Province, China) method with bovine serum albumin as the standard according to the manufacturer's instructions. Four weeks after ADR injection, serum and kidneys were harvested for blood urea nitrogen (BUN), SCR, and histological assessment before sacrifice. BUN and SCR were measured using a Biochemistry Autoanalyzer (Olympus, Tokyo, Japan). To perform the renal histopathology assessment, we removed kidneys rapidly to avoid tissue degeneration. The fresh kidneys were dissected and fixed overnight in 10% neutral phosphate-buffered formalin, dehydrated in alcohol, and then embedded in paraffin. The tissue sections (3-μm thick) were stained with periodic acid-Schiff (PAS) and Masson's stain and viewed using a light microscope. The two senior pathologists were blinded to the identities of the specimens.

Blood was collected from eye artery into tubes and allowed to stand for 30 min. Serum was obtained by centrifugation for 10 min at 3000 r/min and quickly stored at −80°C. Thawed serum (400 μl) was on ice and mixed with 1.0 ml 70% aqueous methanol overnight at 4°C. The following centrifugation at 10,000 ×*g* for

Access this article online

Quick Response Code:

Website: www.cmj.org

DOI: 10.4103/0366-6999.245266

Address for correspondence: Dr. Cai-Li Wang, Department of Nephrology, The First Affiliated Hospital, Baotou Medical College, Baotou, Inner Mongolia 014010, China
E-Mail: wangcaili@btmc.edu.cn

Received: 25-07-2018 **Edited by:** Yuan-Yuan Ji

How to cite this article: Lyu L, Wang CL, Li ZY, Shi YJ, Zhang YH, Mi Y, Hu Z. Serum Metabolic Profiling in a Mouse Model of Adriamycin-Induced Focal Segmental Glomerulosclerosis. Chin Med J 2018;131:2743-6.

10 min, the extracts were adsorbed (CNWBOND Carbon-GCB SPE Cartridge, 250 mg, 3 ml; ANPEL, Shanghai, China, www.anpel.com.cn/cnw) and filtered (SCAA-104, 0.22 μm pore size; ANPEL, Shanghai, China, http://www.anpel.com.cn/) before liquid chromatography-mass spectrometry (LC-MS) analysis.

The sample extracts were analyzed using an LC-electrospray ionization (ESI)-Tandem mass spectrometry (MS/MS) system (UPLC, Shim-pack UFLC SHIMADZU CBM30A system, www.shimadzu.com.cn/; MS, Applied Biosystems 4500Q TRAP, www.appliedbiosystems.com.cn/). The analytical conditions were as follows: UPLC: column, Waters ACQUITY UPLC HSS T3 C18 (1.8 μm, 2.1 mm × 100.0 mm); solvent system, water (0.04% acetic acid): acetonitrile (0.04% acetic acid); gradient program, 100:0 V/V at 0 min, 5:95 V/V at 11.0 min, 5:95 V/V at 12.0 min, 95:5 V/V at 12.1 min, 95:5 V/V at 15.0 min; flow rate, 0.40 ml/min; temperature, 40°C; and injection volume: 5 μl. The effluent was alternatively connected to an ESI-triple quadrupole-linear ion trap (Q TRAP)-MS.

Triple quadrupole scans were acquired on a triple quadrupole-linear ion trap mass spectrometer, API 4500 Q TRAP LC/MS/MS system, equipped with an ESI Turbo Ion-Spray interface, operating in a positive ion mode and controlled by Analyst 1.6 software (https://sciex.com/products/software/analyst-tf-software). The ESI source operation parameters were as follows: ion source, turbo spray; source temperature 550°C; ion spray voltage 5500 V; ion source gas I (GSI), gas II (GSII), curtain gas were set at 55, 60, and 25.0 psi, respectively; the collision gas was high. Instrument tuning and mass calibration were performed with 10 and 100 μmol/L polypropylene glycol solutions in triple quadrupole and LIT modes, respectively. Triple quadrupole scans were acquired as multiple reaction monitoring (MRM) experiments with collision gas (nitrogen) set to 5 psi. Declustering potential (DP) and collision energy (CE) for individual MRM transitions were done with further DP and CE optimization. A specific set of MRM transitions were monitored for each period according to the metabolites eluted within this period.

For normally distributed data, differences of quantitative parameters between groups were analyzed using the *t*-test and descriptive statistics for these data are presented as the mean ± standard deviation. A value of $P < 0.05$ was considered statistically significant. The analysis was performed with SPSS version 13.0 (SPSS Inc., Chicago, IL, USA).

Principal components analysis (PCA) and orthogonal projection to latent structures-discriminant analysis (OPLS-DA) were performed using the AMIX v. 3.9 (Analysis of MIXtures software, Bruker Biospin) software and the SIMCA-P ver. 11.0 software package (Umetrics, Umea, Sweden), respectively. PCA was used first to determine the general intra- and inter-group variation, and OPLS-DA was subsequently performed to maximize the differences in metabolomic profiling. The values of R_2X, R_2Y, and Q_2 were used to estimate the accuracy of the model. R_2X, R_2Y, and Q_2 close to 1 indicated an excellent model that was good for fitness and prediction. The variable selection procedure was based on a modified multi-criteria assessment strategy. Variable importance in the projection (VIP) derived from the OPLS-DA model ranks the importance of each variable for the classification. Those variables with VIP >1.0 were initially considered as statistically significant in the model. We combined fold-change of univariate analysis to further select differential metabolites. Screening criteria were as follows: (1) fold change should be ≥2 or ≤0.5; (2) for biological repeated metabolites samples, VIP ≥1 and *P* value of *t*-test between groups <0.05 were set for enrollment. Hierarchical cluster analysis was performed with R software (www.r-project.org/). The selected differential metabolomic structure and the pathway analysis reference databases were MassBank (http://www.massbank.jp/), KNAPSAcK (http://kanaya.naist.jp/KNApSAcK/), HMDB (http://www.hmdb.ca/),[6] MoTo DB, METLIN (http://metlin.scripps.edu/index.php), and MetaboAnalyst (http://www.metaboanalyst.ca/).

Study details and clinical examination parameters of the normal control and ADR-induced FSGS groups are shown in Table 1. The body weights of ADR-induced FSGS group were significantly lower than those of the normal control group at 21 and 28 days (all $P < 0.05$). The proteinuria in the FSGS group increased gradually and peaked at 28 days ($P < 0.05$) with respect to values in the control group. The levels of SCR and BUN in FSGS group were significantly higher than those in normal control group at 29 days (901.5 ± 57.4 vs. 502.7 ± 51.9 mmol/L; 33.7 ± 5.8 vs. 20.6 ± 3.1 ng/μl, respectively, all $P < 0.05$). We detected changes in kidney histopathology in the ADR-induced FSGS group. There was no apparent damage in the glomeruli, renal tubules, or interstitium in the normal control group as assessed by PAS and Masson's staining [Supplementary Figure 1a and 1b]. However, in the ADR-induced FSGS group, severe pathological lesions were observed, characterized by glomerular swelling, expansion of the renal glomerular capsule space, focal glomerular sclerosis in some of the glomeruli and protein casts in the renal tubular lumens [Supplementary Figure 1c and 1d]. Dramatic tubulointerstitial fibrosis in the FSGS group was revealed by Masson's staining.

We performed metabolomic variations on 11 serum samples obtained from two groups (A group: 5 serum specimens and C group: 6 serum specimens). Mixed quality samples were assigned to each pool to evaluate technical reliability. Representative total ions current from mixed quality control samples is shown in Supplementary Figure 2a and 2b, revealing the intensity of ion current. Multiple peaks from mixed samples present all the detected metabolites, and each spectrum peak represents a detected metabolite. The heatmap presents the clustering and separation of each serum sample from two groups including mixed samples; in particular, the mixed samples are consistent with one another [Supplementary Figure 2c]. The quality control samples from each

Table 1: Comparison of the body weights and urine protein concentrations in mice of ADR-induced FSGS and normal control

Time	Body weight (g)		Urine protein (μg/μl)	
	Normal control	ADR-induced FSGS	Normal control	ADR-induced FSGS
Before administration	23.8 ± 1.1	22.70 ± 0.9	215.9 ± 6.9	225.1 ± 2.9
8th day	25.9 ± 0.8	23.8 ± 1.0*	257.1 ± 13.4	274.5 ± 8.7
15th day	26.5 ± 0.9	25.8 ± 1.3	259.7 ± 7.6	318.0 ± 12.2*
21st day	30.1 ± 1.0	26.4 ± 1.3*	268.0 ± 10.1	399.6 ± 11.4*
28th day	31.3 ± 0.9	27.2 ± 0.6*	278.0 ± 12.1	477.6 ± 13.6*

Data were shown as mean ± SD. *P<0.05 versus normal control group. ADR: Adriamycin; FSGS: Focal segmental glomerulosclerosis. SD: Standard deviation.

group were clustered close together, demonstrating good instrument stability throughout the dansylation LC-MS analysis. PCA score plots analysis for each group as a function of sample clustering and separation was used. The first principal components (PC1; 36.77%) and second PC (PC2; 22.84%) showed that the mixed samples and the normal control group had poor separation, whereas the

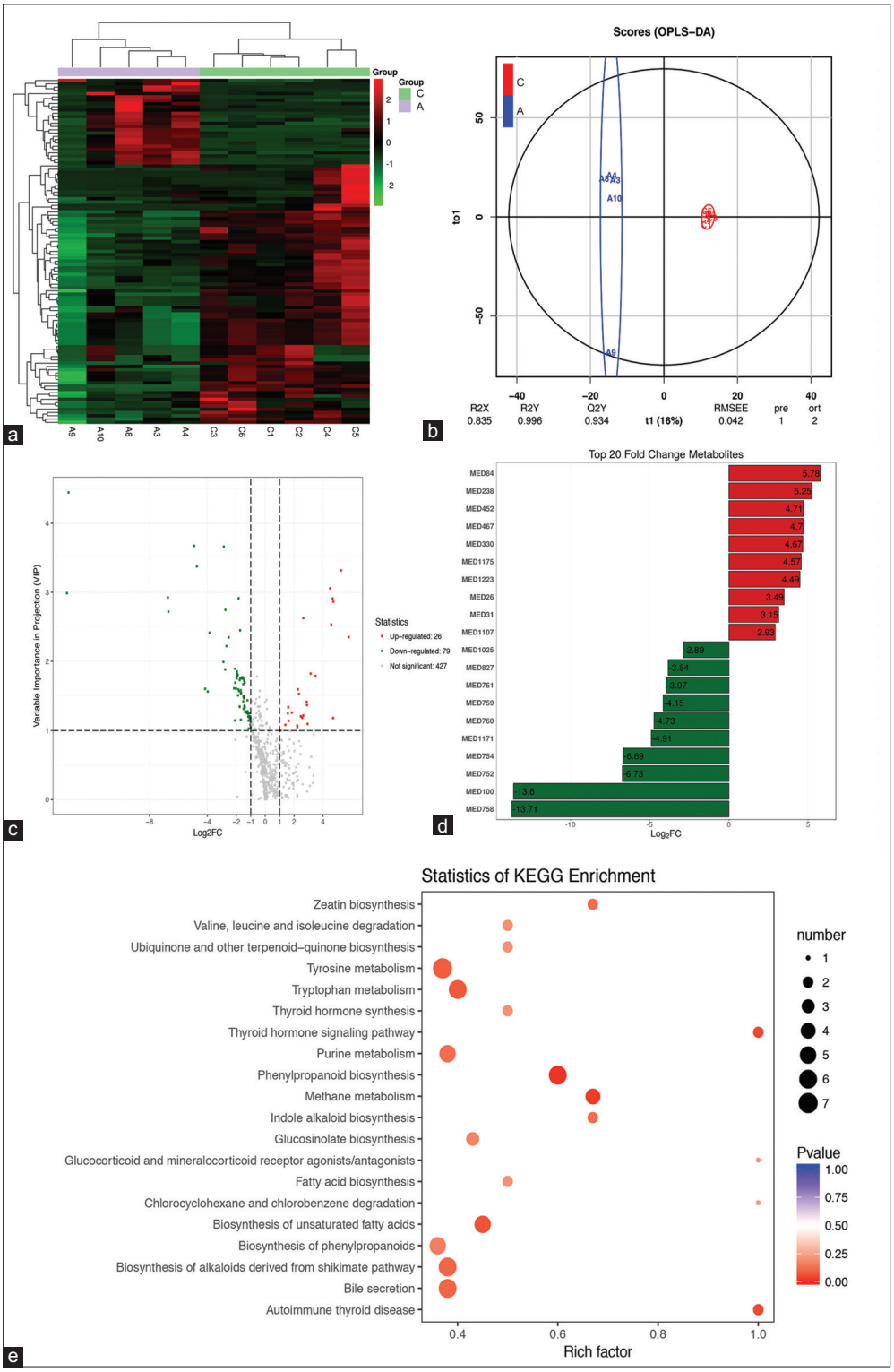

Figure 1: The results of metabolomic variations analysis between the normal control group and the ADR-induced FSGS group. (a) The heatmap presenting the distribution of differential metabolites between ADR-induced FSGS and normal control groups. (b) OPLS-DA plots of serum samples among two groups. (c) Volcano plots presenting the different levels and statistical significance of serum metabolites between the groups. (d) Top twenty differential metabolites by the fold change value transformed by log2 group between the groups. (e) Overview of pathway analysis based on selected serum metabolites from the ADR-induced FSGS group. ADR: Adriamycin; FSGS: Focal segmental glomerulosclerosis; OPLS-DA: Orthogonal projection to latent structures-discriminant analysis.

ADR-induced FSGS group and the normal control group were clearly separated [Supplementary Figure 2d].

Altogether, detailed information of 532 metabolites were identified. We further calibrated the detected mass spectra of certain metabolites in various samples to ensure the accuracy of qualitative and quantitative analysis. Furthermore, we performed a biological repeatability assessment to ensure the reliability of the selected differential metabolites. All data implied that these methods from metabolomics were repeatable.

To assess the integral variations of metabolomics between the ADR-induced FSGS group and the normal control group, we used the heatmap and 3D score plots of related OPLS-DA models [Figure 1a and 1b]. Each row of the heatmap represented a sample. There was a clear dispersion tendency of samples in the ADR-induced FSGS group, indicating that the mice in the ADR-induced FSGS group had more heterogeneity. As depicted by OPLS-DA score plots [Figure 1b], metabolites in the ADR-induced FSGS group compared the normal control group were substantially separated, indicating that the endogenous metabolism of FSGS mice had been significantly altered after ADR induction. The model parameters for the explained variation R_2X and R_2Y were 0.835 and 0.996, respectively, and the predictive capability Q_2 was 0.934, suggesting the robustness of the model.

Subsequently, we identified those metabolites that accounted for the significant separation described above. Hierarchical Pearson clustering analysis revealed obvious differences between the groups. The raw differential metabolites data are accessible in Supplementary Table 1. Volcano plot analysis was used to determine the differential metabolites in the ADR-induced FSGS group compared the normal group [Figure 1c]. The top 20 differential metabolites by fold-change value transformed by log2 between the groups were found [Figure 1d]. The ten downregulated metabolites included palmitoleic acid, l-thyroxine (T4), glycochenodeoxycholic acid, glycodeoxycholic acid, glycocholic acid, inosine diphosphate (IDP), taurochenodeoxycholic acid, tauroursodeoxycholic acid, p-coumaraldehyde, and glycoursodeoxycholic-acid in the ADR-induced FSGS group. In addition to identifying downregulated metabolites, we found ten prominently upregulated metabolites, including trimethylamine-N-oxide (TMAO), pyridoxine, kinetin-9-riboside, p-coumaroyl-cinnamoyl-caffeoyl spermidine, vanillic acid, 3-sialyllactose, n-acetylvaline, l-valine, 3-chloro-l-tyrosine, and 3-methoxy-hydroxyphenyleneglycol sulfate (MHPG-SO4) in the ADR-induced FSGS group.

We further uncovered several potential pathways associated with ADR-induced FSGS using pathway enrichment analysis by Kyoto Encyclopedia of Genes and Genomes database and Metaboanalyst 3.0 analyses (http://www.metaboanalyst.ca). Tyrosine metabolism, biosynthesis of unsaturated fatty acids, bile secretion, and purine metabolism were significantly enriched in the ADR-induced FSGS group [Figure 1e]. This finding suggested that ADR mediated potential changes in these metabolic pathways.

Our study has two major findings. First, we provided a promising viewpoint of the metabolomics perturbation mechanisms associated with kidney damage in ADR-induced FSGS. Second, we identified a subset of differential metabolites and metabolomic pathways involved in the development of ADR-induced FSGS.

Several differential metabolites (pyridoxine, vanillic acid, n-acetylvaline, MHPG-SO4, and palmitoleate) were found to possibly evolve into FSGS and may be peculiar to ADR-induced FSGS in this study. Furthermore, we found that the serum concentration of the several differential metabolites (T4, IDP, 3-CLY, TMAO, l-valine, some bile acid metabolites, and its derivatives) were substantially altered in the ADR-induced FSGS group, all of which were previously reported to be associated with chronic kidney disease. Therefore, we suggest that these metabolites may contribute to kidney damage, but may not appear to be specific metabolites for ADR-induced FSGS. Finally, bile acid metabolism, purine metabolism, branched chain amino acids metabolism, tyrosine metabolism, and unsaturated fatty acids may be involved in the development of ADR-induced FSGS.

There are some limitations of this study. First, we only showed findings at the stage of well-established FSGS in mice, not at various stages of the disease. Therefore, our study could not reveal clear causative relationships between abnormal metabolites and FSGS development. Second, the serum levels of metabolites were affected by food intake, because mice injected with ADR had loss of appetite.

In conclusion, a panel of differential serum metabolites and potential metabolic pathways were associated with kidney damage in ADR-induced FSGS mice models.

Supplementary information is linked to the online version of the paper on the Chinese Medical Journal website.

Financial support and sponsorship

This study was supported by grants from the National Natural Science Fund (No. 81260122 and 81760135).

Conflicts of interest

There are no conflicts of interest.

References

1. Gbadegesin R, Lavin P, Foreman J, Winn M. Pathogenesis and therapy of focal segmental glomerulosclerosis: An update. Pediatr Nephrol 2011;26:1001-15. doi: 10.1007/s00467-010-1692-x.
2. De Vriese AS, Sethi S, Nath KA, Glassock RJ, Fervenza FC. Differentiating primary, genetic, and secondary FSGS in adults: A clinicopathologic approach. J Am Soc Nephrol 2018;29:759-74. doi: 10.1681/ASN.2017090958.
3. Wang YM, Wang Y, Harris DC, Alexander SI, Lee VW. Adriamycin nephropathy in BALB/c mice. Curr Protoc Immunol 2015;108:15.28.1-6. doi: 10.1002/0471142735.im1528s108.
4. Fogo AB. Animal models of FSGS: Lessons for pathogenesis and treatment. Semin Nephrol 2003;23:161-71. doi: 10.1053/snep.2003.50015.
5. Okasora T, Takikawa T, Utsunomiya Y, Senoh I, Hayashibara H, Shiraki K, *et al.* Suppressive effect of superoxide dismutase on adriamycin nephropathy. Nephron 1992;60:199-203. doi: 10.1159/000186739.
6. Kalim S, Rhee EP. An overview of renal metabolomics. Kidney Int 2017;91:61-9. doi: 10.1016/j.kint.2016.08.021.

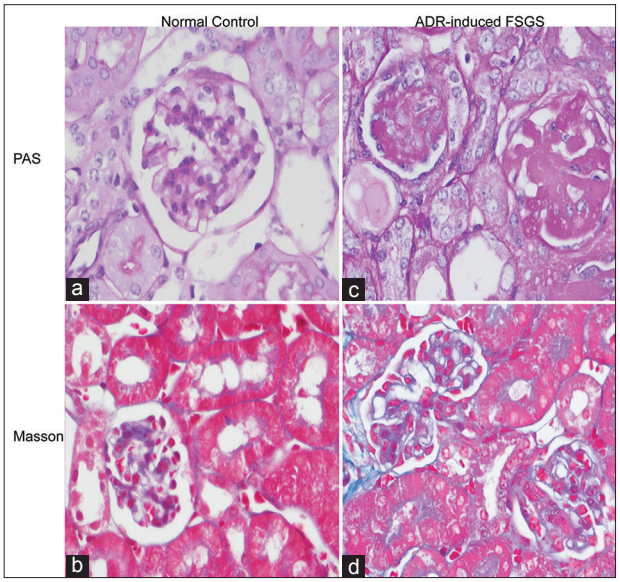

Supplementary Figure 1: Kidney pathohistology using PAS and Masson staining. (a and b) Kidney pathological changes from the normal control group. (c and d) Kidney pathological changes from the ADR induced-FSGS group (×400). ADR: Adriamycin; FSGS: Focal segmental glomerulosclerosis; PAS: Periodic acid–Schiff.

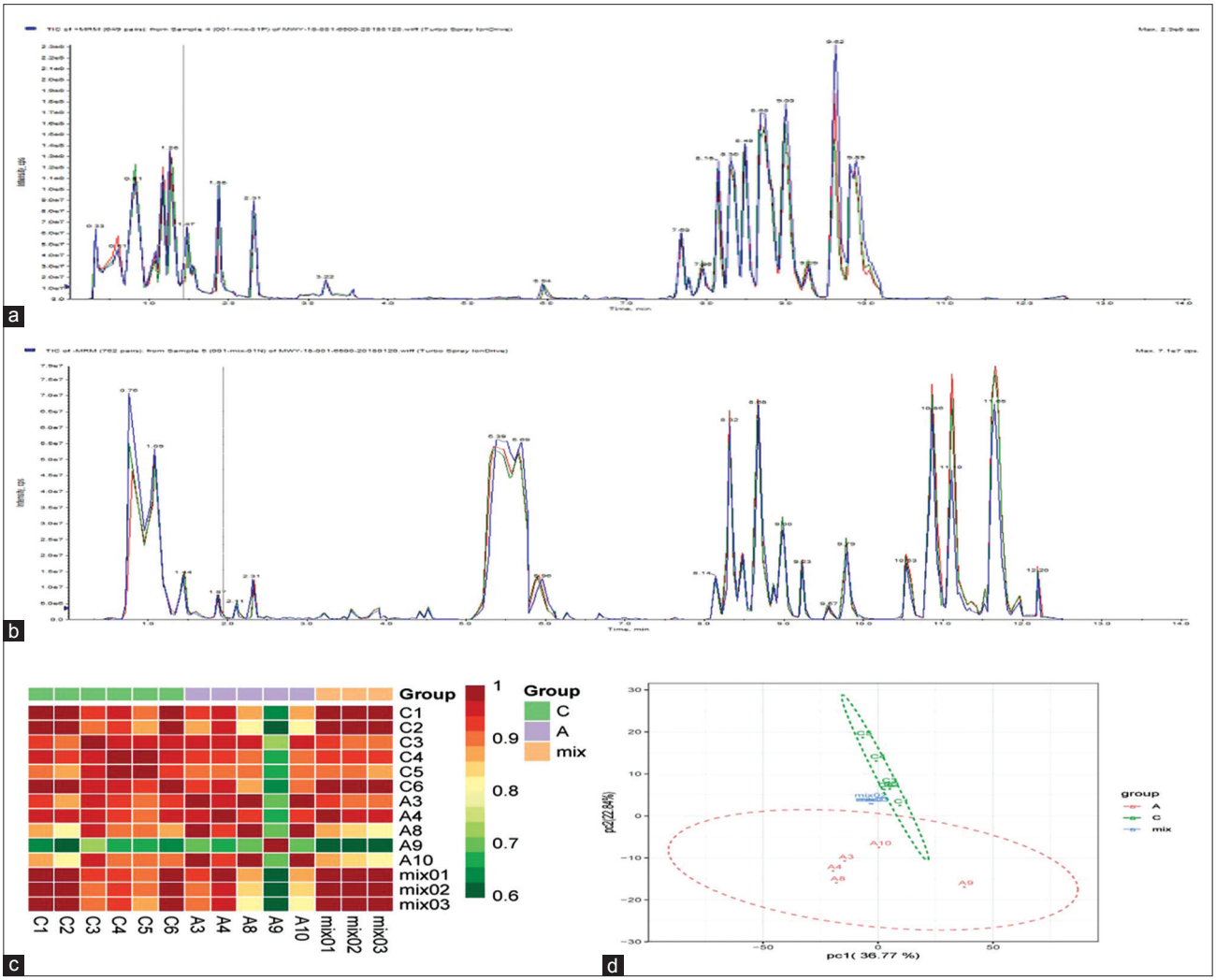

Supplementary Figure 2: The QC of serum metabolomics between groups. (a) The superposition of positive TIC graph detected by QC; (b) the superposition of negative TIC graph detected by QC; (c) the biological repeatability assessment between samples in the observation group; (d) score plots of PCA analysis for QC and samples. QC: Quality control; TIC: Total ions current; PCA: Principal components analysis.